Testing the GAGG Scintillator Crystal and the Search for Neutrinoless Double Beta Decay

Emma Codianne
Department of Physics and Astronomy, School of Natural Sciences, Rice University
Yokoyama-Nakajima Group, Department of Physics, The University of Tokyo
(Dated: August 27, 2023)

***Abstract* – The search for neutrinoless double beta decay ($0\nu\beta\beta$) has garnered interest as a lepton-number violating process that if observed, would confirm that neutrinos are Majorana fermions, or particles that are their own antiparticles. This would mean that neutrinos and antineutrinos are indistinguishable, however, the radioactive decay process of $0\nu\beta\beta$ is difficult to observe. The purpose of this study is to examine the radio impurity of the GAGG scintillator crystal to differentiate between internal and external decay of ^{214}Bi, and calculate a lower limit on the half-life of ^{160}Gd $0\nu\beta\beta$. Studying and reducing the radio impurity of this scintillator could make it easier to improve the quality of the crystal in hopes of observing $0\nu\beta\beta$.**

I. INTRODUCTION

A. Neutrinos

The neutrino is an electrically neutral elementary particle with such a small rest mass that it was long thought to be zero. Neutrinos are the most abundant particles in the universe that have mass, and often pass through matter undetected. They are created by different types of radioactive decays, including beta decays of nuclei, supernovae, and nuclear reactions in star cores. There are three flavors of neutrinos, the electron (ν_e), muon (ν_μ), and tau (ν_τ) neutrino. In 2015, it was proven that neutrinos oscillate between the three flavors, and therefore, must have mass [1]. Currently, it is unknown whether neutrinos are Dirac or Majorana fermions. Both types of fermion have spin 1/2, but Dirac particles are distinguishable from their antiparticles, while Majorana particles are not.

B. Neutrinoless Double Beta Decay

If neutrinos are indeed Majorana fermions, meaning that neutrinos and antineutrinos are indistinguishable, processes that violate lepton-number conservation would be allowed. Notably, the observation of neutrinoless double beta decay ($0\nu\beta\beta$) would prove that neutrinos are Majorana particles [2]. Double beta decay occurs when certain isotopes decay, and two electrons and two neutrinos are emitted. If neutrinos are their own antiparticles, they could self-annihilate during this process, resulting in neutrinoless double beta decay:

$$2n \rightarrow 2p + 2e^- + 0\nu_e \tag{1}$$

Due to the small mass of neutrinos, the long half-life of $0\nu\beta\beta$, and background radiation that can produce electrons in a similar megaelectronvolt energy range as $0\nu\beta\beta$, the process of $0\nu\beta\beta$is difficult to observe.

The decay rate of neutrinoless double beta decay is as follows:

$$(T_{1/2}^{0\nu})^{-1} = G^{0\nu}|M^{0\nu}|m_{\beta\beta}^2 \tag{2}$$

where $m_{\beta\beta}$ is the Majorana mass.

C. Scintillator Crystals

Scintillators are materials capable of converting high-energy radiation, such as gamma or electron energy, into photons. These materials are useful in detection and spectroscopy of various radiations, as they convert high energy into visible or near-visible light. Scintillators come in many different forms, including crystals, liquid organic solutions, thin films, and plastic scintillators [3]. This study focuses on the use of a type of crystal scintillator, the GAGG (Gadolinium Aluminium Gallium Garnet) crystal. In the process of scintillation, the crystal absorbs energy from high-energy electrons, such as those produced from gamma rays, which in turn excites electrons in the scintillator. When these electrons are de-excited, scintillation photons in the visible spectrum are emitted. Since the number of scintillation photons emitted is almost proportional to the incident energy, high energy radiation can be measured by examining the total intensity of scintillation photons.

D. Photomultiplier Tubes

Photomultiplier tubes (PMTs) are devices that convert extremely weak light output into usable electrical signals. PMTs are used in scintillation counting, optical spectroscopy, laser measurements, and astronomy. In a PMT, photons first pass through the photocathode of the device and are converted into photoelectrons. The number of photoelectrons depends on the incident photons, and the quantum efficiency (QE) of a photocathode can be defined as:

$$\text{QE} = \frac{\text{number of photoelectrons emitted}}{\text{number of incident photons}} \tag{3}$$

Typical PMTs exhibit a quantum efficiency of 20-30%. Photoelectrons can then pass through the electron multiplier structure, strike the surfaces of the series of dynodes, and be amplified to about 10^6 - 10^7 electrons. This is enough to serve as a charge signal for the original scintillation event, and is collected at the anode [3]. In this experiment, a PMT and waveform digitizer are used in combination with the GAGG scintillator crystal in order to collect data and analyze radioactive impurities within the crystal.

II. EXPERIMENTAL SETUP

A cerium-doped gadolinium crystal scintillator was used in the following measurements.

A. GAGG Crystal

The GAGG crystal used in the following measurements has a composition of $(Gd_{0.99}CeO_{0.01})_3Al_2Ga_3O_{12}$ and dimensions listed in Table I. The crystal was grown by the Institute for Materials Research at Tohoku University in Sendai, Japan. The sample is made with high-purity gadolinium in its efforts to search for neutrinoless double beta decay. Prior to the use of this crystal in measurements, it was cleaned with an acid treatment to further improve its purity.

TABLE I
GAGG Crystal Dimensions

Radius	Thickness	Mass	Density
2.3 cm	1 cm	26.33 g	6.34 g/cm^3

Fig. 1. GAGG crystal of composition $(Gd_{0.99}CeO_{0.01})_3Al_2Ga_3O_{12}$.

B. Laboratory Setup

Equipment used in this research includes the Hamamatsu Photomultiplier Tube H11934 Series, and the CAEN DT5725 Waveform Digitizer. The CAEN Digitizer is equipped with a sampling rate of 250 Ms/s and 14-bit resolution.

Fig. 2. CAEN DT5725 Wave Digitizer.

In order to take measurements, the GAGG crystal was secured to the photocathode-side of the PMT with electrical tape. In between the crystal and surface of the PMT, optical grease was applied to prevent reflections and improve transmission of light. The whole crystal and PMT were then once again wrapped in electrical tape to ensure that no external light affected the measurements. Before taking data, the setup was left for a few days to help lower background noise from when the GAGG crystal was exposed to light.

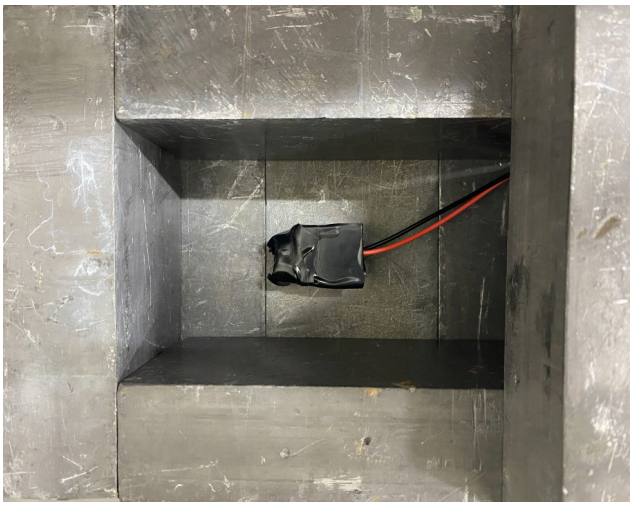

Fig. 3. GAGG crystal attached to Hamamatsu photomultiplier tube with lead shielding.

As pictured above, lead shielding was added while taking measurements to further reduce background radiation. Ten lead bricks of dimensions 5 cm x 10 cm x 20 cm were placed around the PMT to fully enclose the setup. The PMT was connected to both the waveform digitizer and a high voltage supply set at -900 V.

C. Waveform Analysis

After collecting data using the GAGG crystal, PMT, high voltage supply, and waveform digitizer in combination, the resultant waveform of each event recorded was plotted and integrated for further analysis. In order to calculate charge and energy distributions for the recorded events, pedestal values of the waveforms and integration windows were defined, where each count on a plotted waveform is equal to 4 ns. The pedestal was calculated by taking the mean of the first 100 counts of the waveform to reduce the amount of background noise included in the integral calculations. In Figure 4, the pedestal value is depicted by the green line.

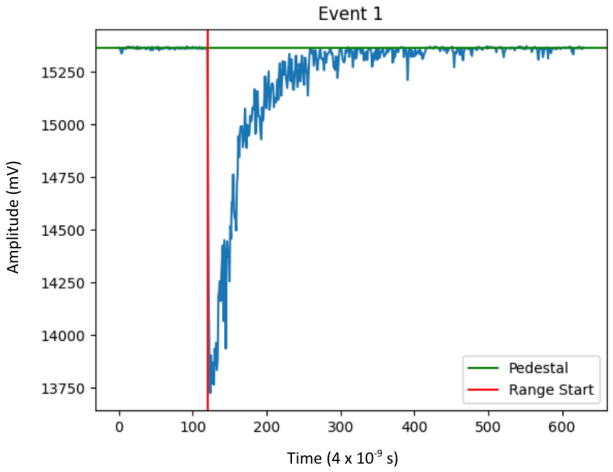

Fig. 4. Sample waveform plotted using the CAEN Wave Digitizer. The pedestal for this event is drawn in green, and the starting point of the integration window is drawn in red.

The integral window was defined as the range from the starting point of the prompt signal minus 10 counts, to 200 counts after this point, with one count equal to 4 ns. The starting point of each peak was found by implementing a height threshold to differentiate peaks from background radiation, where a prompt signal peak must reach below an amplitude of 15,200 mV. The starting point of a sample waveform is depicted in red in Figure 4. Using the time window described, each recorded waveform was integrated to calculate charge and energy distributions of the data.

D. Energy Calibration

Before taking measurements, energy calibration was conducted using ^{137}Cs and ^{60}Co radioactive isotopes. To perform energy calibration, peaks found from the charge distributions of the two isotopes were plotted against the known energies of ^{137}Cs and ^{60}Co to obtain a linear fit. Using the inverse of this fit, the energy distributions of the two isotopes were then plotted and compared to the respective energy peaks based on the decay diagrams. The decay diagrams and energy spectra are shown in Figure 5 and 6, respectively.

One implication of the energy calibration in this research is that the obtained energy peaks of ^{137}Cs and ^{60}Co shifted as calibration measurements were taken over the course of a couple weeks, shown in Table II. The peaks gradually shifted away from the known 0.662 MeV peak of ^{137}Cs, and the 1.173 MeV and 1.333 MeV peaks of ^{60}Co. The reason for these shifts in energy peaks is unknown, though possibly caused by movement of the GAGG crystal or optical grease attached to the PMT surface. Time-dependent calibration would be more appropriate in this situation.

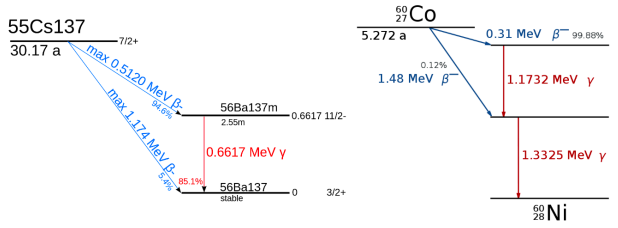

Fig. 5. Decay chains of ^{137}Cs (left) and ^{60}Co (right).

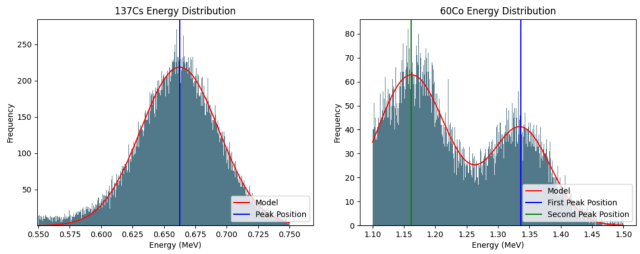

Fig. 6. Energy distributions of ^{137}Cs (left) and ^{60}Co (right). ^{137}Cs had a fitted peak at 0.6626 MeV, and ^{60}Co had peaks at 1.3361 MeV and 1.1619 MeV.

TABLE II
Energy Calibration Peak Shifts

Date	^{137}Cs Peak	^{60}Co First Peak	^{60}Co Second Peak
Jul. 13	0.6597569 MeV	1.1501743 MeV	1.3410324 MeV
Jul. 15	0.6497914 MeV	1.1499489 MeV	1.3080945 MeV
Jul. 20	0.5785271 MeV	0.9968762 MeV	1.143068 MeV
Jul. 24	0.558307 MeV	0.9795780 MeV	1.1359867 MeV

III. RESULTS

In this study, measurement time for all of the following data was 182 hours, or 6.5 x 10^5 seconds, which collected 12,905 events.

A. Measuring Radioactive Impurity

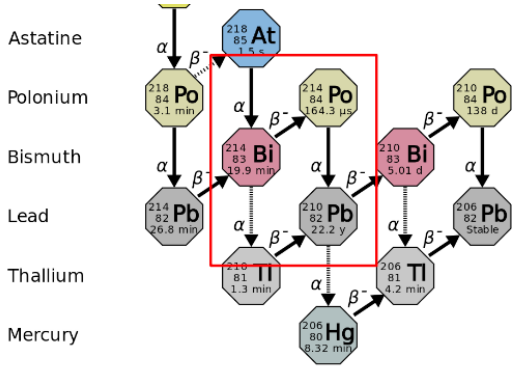

Fig. 7. Decay chain of ^{214}Bi.

The ^{214}Bi $\rightarrow$ ^{214}Po $\rightarrow$ ^{210}Pb decay chain is used in this experiment to examine the radio impurity of the GAGG crystal. This small decay chain consists of two different types of decay: ^{214}Bi $\rightarrow$ ^{214}Po is beta decay, while ^{214}Po $\rightarrow$ ^{210}Pb is alpha decay. In this study, the presence of both parts of the decay chain would mean multiple peaks (both prompt and delayed signals) in the observed waveforms from the PMT and waveform digitizer. In order to study the radio impurity of the GAGG crystal, the internal and external decay of ^{214}Bi need to be differentiated. This will help illuminate whether the background noise seen in data is originating from environmental radiation or impurities in the crystal itself. Additionally, both parts of the decay chain need to be analyzed, since using the prompt signal peaks of waveforms alone cannot determine whether the decay is from background or $0\nu\beta\beta$, as $0\nu\beta\beta$ does not exhibit multiple peaks.

B. Pulse Shape Analysis

This study's main measurement was conducted to search for $0\nu\beta\beta$ and examine radioactive impurities within the GAGG crystal, so no additional isotopes were used like with energy calibration. The energy distribution of the environmental radiation measurement is plotted in Figure 8, with the peaks

of naturally-occurring radiation labeled. The peak of ^{40}K is expected around 1.46 MeV and ^{208}Tl, while slightly harder to observe, is at 2.6 MeV. The region where $0\nu\beta\beta$ is expected to occur for ^{160}Gd (natural abundance $\approx 22\%$) is also marked at 1.73 MeV [4]. No $0\nu\beta\beta$ peak was observed in this measurement around the region.

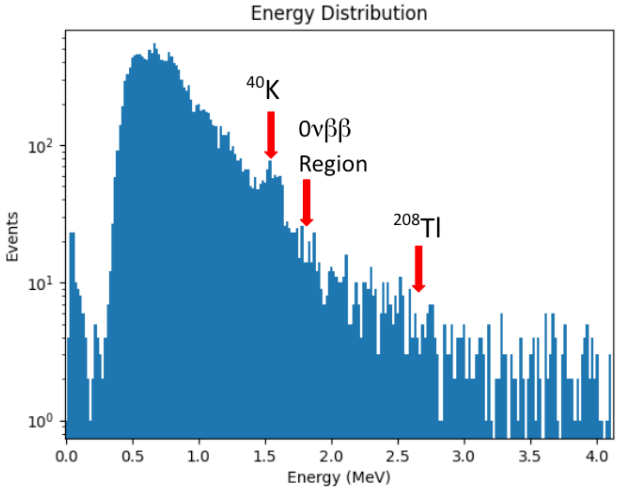

Fig. 8. Energy distribution of environmental radiation measurement over 182 hours. The known energies of ^{40}K and ^{208}Tl are labeled at 1.46 MeV and 2.6 MeV, respectively. The region where $0\nu\beta\beta$ is expected to occur around 1.73 MeV is also noted.

Looking at the first part of the ^{214}Bi decay chain, from ^{214}Bi to ^{214}Po, this prompt signal region can be analyzed to distinguish between different pulse shapes. This can be done by examining different time constants between γ and α decays. Analysis was conducted using Python, calculating the peak-to-tail ratio of each prompt signal peak from the measurement data. In order to calculate this ratio, two integrals were taken for each prompt signal at a chosen cutoff and compared using:

$$\text{ratio} = \frac{\text{peak integral}}{\text{tail integral}} \tag{4}$$

To define the peak and tail integral ranges, the time widths were chosen based on the plotted waveforms, using the same algorithm described in the Waveform Analysis section to identify the starting points of prompt signals. The peak integral of the peak-to-tail ratio was defined as the range from the starting point of the prompt signal to 100 counts (or 400 ns) after this point. Then, the tail integral was defined as the range from the previous end point to 500 counts (or 2000 ns) afterwards. A larger ratio indicated that the peak is from γ sources, which exhibit a sharper waveform. On the other hand, a smaller ratio implied peaks occurring from α sources with a smaller time constant. Two example waveforms and the integral cutoff are shown in Figure 9.

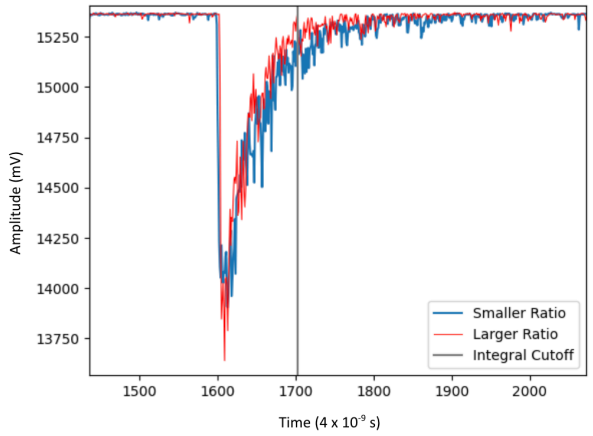

Fig. 9. The first peaks of two waveforms are plotted, along with the chosen integral cutoff value to perform pulse shape discrimination. The blue waveform was calculated to have a smaller integral ratio and is indicative of alpha decay, while the red waveform is from gamma sources.

From these calculated integral ratios, pulse shape discrimination of the prompt signal peaks of recorded waveforms can be analyzed by looking at energy distributions. As shown in Figure 10, the integral ratios for the environmental radiation measurement can be plotted against energy and shows two peaks. The smaller peak around a smaller integral ratio of 4-5 indicates prompt signals resulting from alpha decay. To confirm that the calculations correctly indicate the type of source based on the integral ratios, Figure 11 shows the calibration measurement conducted with ^{137}Cs. As expected, there is only one clear peak since the observed waveforms should occur from the external γ source.

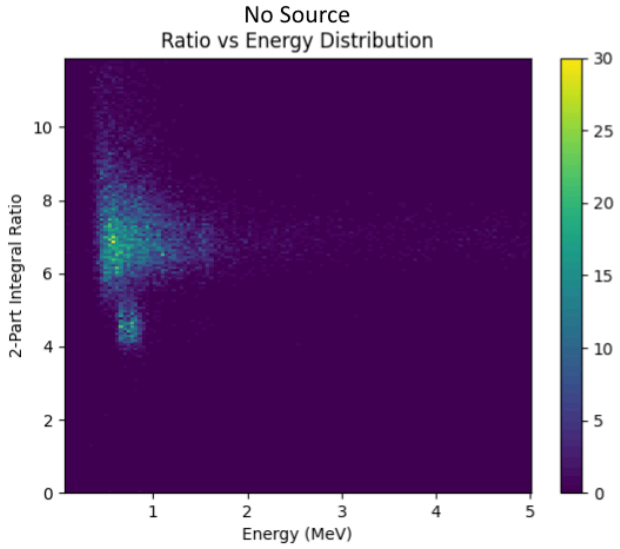

Fig. 10. 2D histogram plotting calculated peak-to-tail integral ratios against energy for the GAGG crystal environmental radiation measurement.

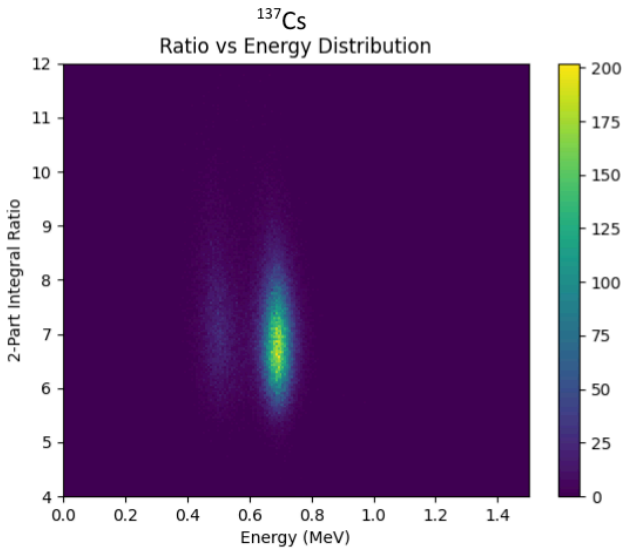

Fig. 11. 2D histogram plotting calculated peak-to-tail integral ratios against energy for calibration data using the ^{137}Cs isotope.

C. Half-Life Limit of $0\nu\beta\beta$

^{160}Gd is a nuclei candidate for double beta decay due to its lower theoretical half-life, and because its energy region for $0\nu\beta\beta$ could possibly be free from $2\nu\beta\beta$ background decays. In addition, the relatively large natural abundance of ^{160}Gd at 21.9% makes it a promising candidate for $2\nu\beta\beta$ [4].

An experiment conducted by F.A. Danevich at the Solotvina Underground Laboratory using the GSO (Gd_2SiO_5:Ce) scintillator crystal calculated the lower-limit on the half-life of $0\nu\beta\beta$ of ^{160}Gd to be 1.3 x 10^{21} years [4].

In this study, the lower-limit on the half-life of neutrinoless double beta decay is calculated using the same equation as Danevich:

$$T_{1/2} = ln2 \cdot \eta \cdot N \cdot t / lim(S) \tag{5}$$

where:

$T_{1/2}$ - lower-limit of the half-life;

η - detection efficiency;

N - number of ^{160}Gd nuclei in the crystal;

t - measurement time;

$lim(S)$- the maximum number of $0\nu\beta\beta$ events that can be excluded with a given confidence level based on the data

To find the value of lim(S), Danevich describes two approaches to calculation. First is the "one σ approach," where the number of excluded real events that could be invisible in the spectrum is estimated as the square root of the number of background event counts in a chosen energy range. Second is the standard least squares method, in which the energy distribution in the vicinity of the targeted peak was fitted with the sum of the background model and the $0\nu\beta\beta$ decay peak being searched for. The "one σ approach" was used in this study.

In this study's calculation of the $0\nu\beta\beta$ half-life limit,

- η = 1 (assuming perfect detection efficiency)
- N = 3.76 x 10^{21} nuclei of ^{160}Gd in GAGG crystal
- t = 182 hours (6.5 x 10^5 seconds)
- $lim(S) = \sqrt{122}$

where $lim(S)$ was calculated using σ from the Gaussian fit of the ^{137}Cs energy calibration, and extrapolated to the $0\nu\beta\beta$ peak at 1.73 MeV. From this, the chosen energy range was taken to be 1.68 MeV to 1.78 MeV, and 122 background events were found in this region. With this information, the lower-limit of the $0\nu\beta\beta$ half-life was calculated to be:

$$T_{1/2}(0\nu\beta\beta) \geq 4.899 \times 10^{18} \text{ years} \tag{6}$$

D. Investigation of Radioactive Impurity

When looking at the ^{214}Bi decay chain, this section of the study aims to distinguish and analyze delayed signal peaks of the recorded waveforms that follow the prompt signal. This corresponds to the ^{214}Po $\rightarrow$ ^{210}Pb decay that occurs less frequently. Using the same process described above for the prompt signals, the energy distribution, integral ratios, and subsequent 2D histogram plotting the two were calculated for delayed signals. On the waveform plots, a height threshold was implemented to filter out background noise from being counted as delayed signal peaks. Figure 12, the plot of delayed signal integral ratios against energy, also exhibits two peaks, suggesting two different pulse shapes. However, it is noteworthy to add that the same plot should also be made using the integral ratios as the filter to detect possible α decay peaks rather than a height threshold.

Figure 13 shows the histogram plot of time differences between prompt and delayed signals. Removing the background noise, an exponential decay relationship is expected for the peak time differences, as the second decay of ^{214}Bi (^{214}Po $\rightarrow$ ^{210}Pb) has a known half-life of 164.2 μs.

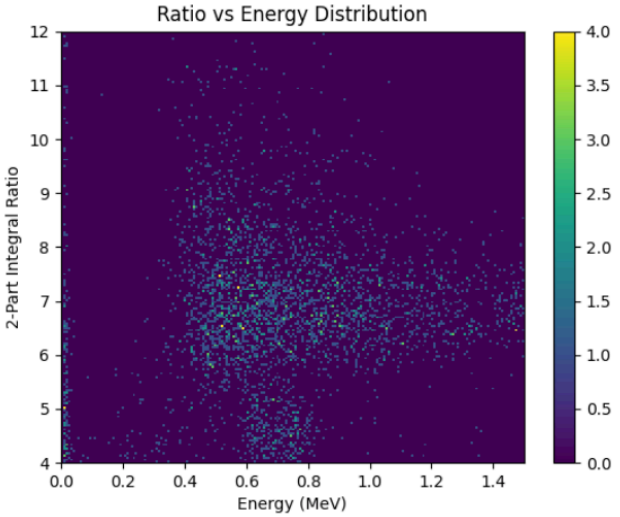

Fig. 12. 2D histogram plotting calculated peak-to-tail integral ratios against energy for detected multiple peaks in the observed waveforms.

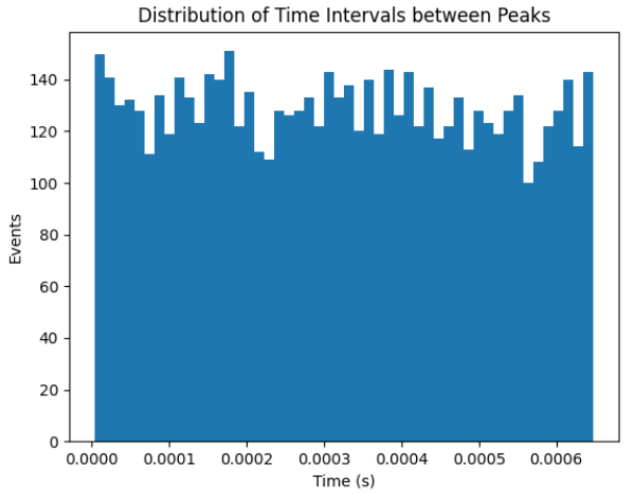

Fig. 13. Histogram of the time difference between prompt signal and delayed signal peaks that are above a certain threshold height to distinguish from background noise.

IV. DISCUSSION AND FURTHER WORK

When examining the time differences between prompt and delayed signals, an exponentially decreasing relationship in the histogram would indicate the ^{214}Bi decay process. However, Figure 13 does not exhibit a clear exponential decay, which suggests that no significant signal of ^{214}Bi decay was found in this study of the GAGG crystal. This would mean that the crystal's purity has improved and there are less effects from background.

In the analysis of radioactive impurity using delayed signal peaks, the threshold for determining multiple peaks can be refined to better filter out background noise. In doing so, the histogram of time differences between peaks can be more clearly plotted. Additionally, in a similar manner to testing pulse shape differences with a γ source (in this study, ^{137}Cs), using an α source when measuring the GAGG crystal can be used to confirm whether peaks calculated to occur from α decay are indeed from α particles. As noted in the Experimental Setup section, the implementation of time-dependent energy calibration could also be used to combat the shifting energy peaks observed before taking measurements.

V. CONCLUSIONS

In this study, it was demonstrated that the GAGG scintillator crystal has the ability to measure individual γ rays with accuracy, as in the case of ^{137}Cs and ^{60}Co. With the 26.33g crystal, the lower-limit on the half-life of ^{160}Gd $0\nu\beta\beta$ was calculated to be 4.899 x 10^{18} years. The radio impurities of the GAGG crystal were further examined in hopes of improving the crystal's purity, notably looking at delayed signal peaks in the recorded waveforms. The time differences calculated between prompt and delayed signals indicates no significant evidence for ^{214}Bi decay in the GAGG crystal, which would mean a more effective crystal scintillator in hopes of observing $0\nu\beta\beta$.

ACKNOWLEDGEMENT

I would like to thank Professors Masashi Yokoyama and Yasuhiro Nakajima for giving me the opportunity to participate in their laboratory this summer, and a special thanks to Prof. Nakajima for his patient guidance throughout my research. I would also like to thank all of the students in the Yokoyama-Nakajima Group for their kind welcome and assistance, the staff members of the University of Tokyo International Team and Graduate School of Science in planning UTRIP, and Friends of UTokyo, Inc. for their generous scholarship and support.

REFERENCES

[1] A. Taroni, "Nobel Prize 2015: Kajita and McDonald", *Nature Physics 11, 891*, 2015.

[2] G. Gratta, "Search for neutrinoless double-β decay", *Nature 538, 48-49*, 2016.

[3] G. F. Knoll, *Radiation Detection and Measurement*, Wiley, 2010.

[4] F. Danevich, "Quest for double beta decay of ^{160}Gd and Ce isotopes", *Nuclear Physics A 694, 375-391*, 2001.